JULY 12–16 2020 VIRTUAL
JOINT AAPM | COMP MEETING
EASTERN TIME [GMT-4]

Dark Field Proton Radiography: A Proof of Principle

MS Freeman, JC Allison, EF Aulwes, M Espy, PE Magnelind, FG Mariam, JJ Medina, WZ Meijer, FE Merrill, LP Neukirch, T Schurman, RB Sidebottom, Z Tang, FR Trouw, D Tupa, J Tybo
Los Alamos National Laboratory, Los Alamos, NM

Los Alamos NATIONAL LABORATORY EST. 1943

INTRODUCTION

Dark field proton radiography combines the principles of Schlieren optical imaging,[1] or dark field X-radiography,[2] with lens-based proton radiography.[3] By exploiting the conditions at a Fourier plane upstream of the object, where the angle of a proton's trajectory is mapped to position, protons beyond a certain angular cut angle are removed from the beam. Downstream of the object, at a second Fourier plane, an inverse collimator,[4] of the same angular cut angle, is placed. These two Fourier planes effectively map to each other, and thus, without an object at the object plane, no protons are transmitted through the system. By placing an object at the object location, additional scatter is introduced to the proton distribution, allowing for transmission through the downstream inverse collimator. Imaging in this way allows for the removal of many of the protons that carry little information from the system, before they interact with the patient, allowing for images to be acquired with less dose. Such a system could allow for the instantaneous measure of patient stopping power with reduced dose.

AIM

The aim of this study is to provide an instantaneous measure of proton stopping power, with the highest amount of information per dose deposition possible. Dark field proton radiography has the ability to provide high quality proton stopping power information, with a reduction to dose delivered. By removing the highly scattered protons before the beam reaches the patient, the amount of protons used to acquire an image is decreased, while the removal of the least scattered protons downstream of the patient, protons that carry proportionately very little information are removed from the system, reducing noise.

METHOD

A dark field condition was created by applying a pre- and post-collimation scheme to the high energy proton radiography facility at Los Alamos Neutron Science Center. With a cut angle that removes protons of less than 2 mrad of scatter upstream, and more than 2 mrad of scatter downstream, the default is to have zero transmission until an object is presented. Proton radiographs are acquired of a 20-cm thick acrylic phantom to compare between a conventional proton radiographic setup (at 5 mrad acceptance) and the dark field proton radiographic setup.

A schematic of the dark field radiography setup is illustrated in Fig. 1. All protons that are permitted beyond the upstream Fourier plane, are then stopped by the downstream Fourier plane, as shown in Fig. 2. If an object is introduced that adds additional scatter to the proton distribution, transmission is permitted beyond the downstream Fourier plane.

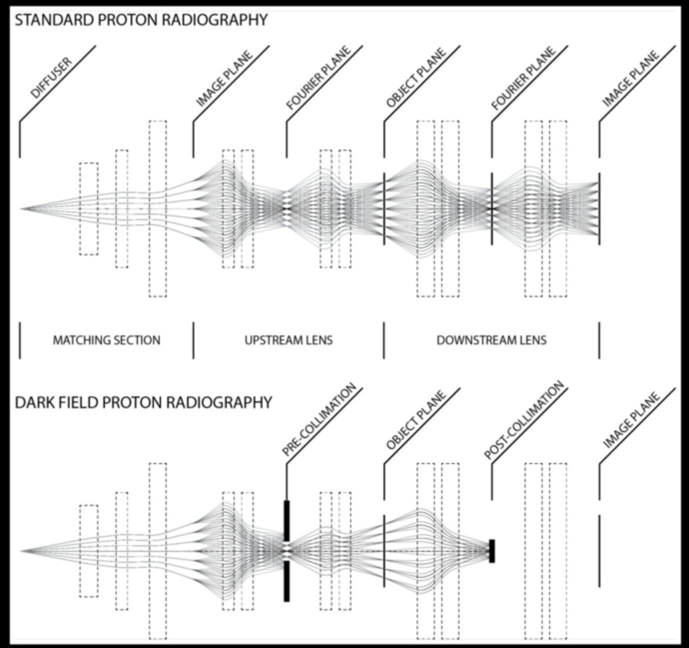

Figure 1: Schematic comparing traditional lens-based proton radiography to the dark field condition. Objects introduced at the object plane permit transmittance beyond the post collimation stage.

RESULTS

In Fig. 2, flat field images are shown, in which an image is acquired with no object present. For the standard radiography setup, the beam distribution is Gaussian in nature, where transmission decreases with the introduction of an object. In the dark field version of the no-object image, transmission defaults to zero, where transmission now goes *up* in the case of material present at the object location.

Dark field proton radiographs demonstrate an SNR improvement of a factor of 2 over conventional proton radiography. Sensitivity to changes in water equivalent path length in 20-cm of acrylic was improved from 1% with standard proton radiography, to 0.25% with dark field proton radiography, as shown in Fig. 3.

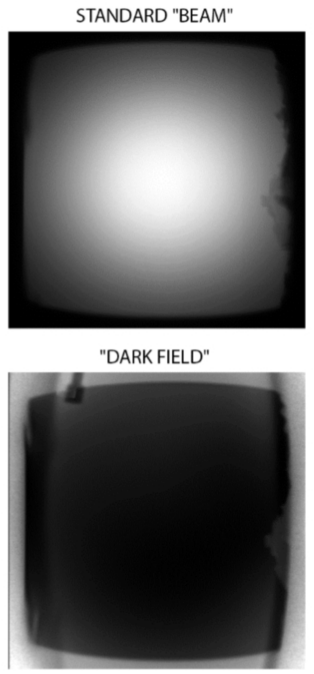

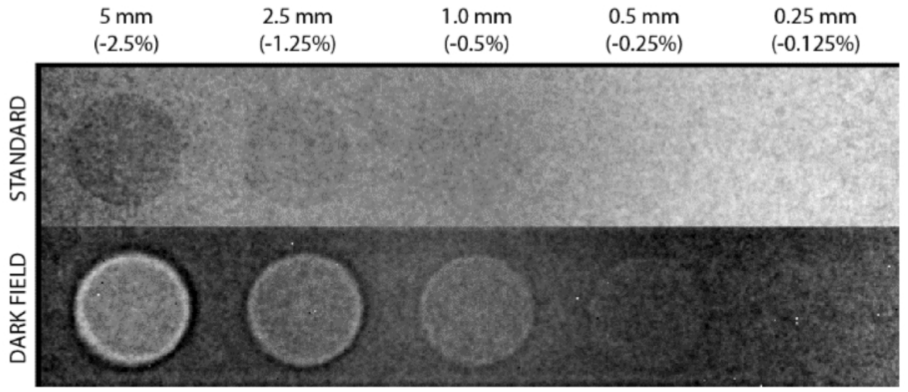

Figure 3: These radiographs are acquired through a block of acrylic, 20-cm thick. 1-cm diameter holes are drilled to the depths as labeled, with percent density change labeled (in parentheses). Standard radiography discerns to roughly the (expected) 1% sensitivity level. Dark field proton radiography detected down to the 0.25% sensitivity.

Figure 2: A standard proton radiography flat field, at top, demonstrates a Gaussian profile that represents 100% transmission. By comparison, in the dark field configuration, there is no transmission through the system from protons that are not scattered by an object.

CONCLUSIONS

Initial results indicate that the system provides a sensitivity improvement to subtle areal density variations within thick objects. This is likely due to two effects: the removal of highly scattered protons before the object location, and the removal of unscattered protons after the object location. The protons remaining carry the highest amount of radiographic information and a lower amount of noise. This could have implications for beam's-eye-view image guidance for proton therapy, or for treatment planning, where increasingly accurate measures of water equivalent path length translate directly into increased estimates of dose deposition.

Future work will compare this system against a 230-MeV, single-proton counting, two-detector proton radiography system, in simulation.

REFERENCES

[1] Schardin, Hubert. "Schlieren methods and their application." *Ergbnisse der Exakten Naturwissenschaften* 20 (1942): 303-439.

[2] Pfeiffer, Franz, et al. "Hard-X-ray dark-field imaging using a grating interferometer." *Nature materials* 7.2 (2008): 134-137.

[3] King, N. S. P., et al. "An 800-MeV proton radiography facility for dynamic experiments." *Nuclear Instruments and Methods in Physics Research Section A: Accelerators, Spectrometers, Detectors and Associated Equipment* 424.1 (1999): 84-91.

[4] Freeman, Matthew S., et al. "Inverse-collimated proton radiography for imaging thin materials." *Review of Scientific Instruments* 88.1 (2017): 013709.

ACKNOWLEDGEMENTS

This work was supported by the US Department of Energy through the Los Alamos National Laboratory. Los Alamos National Laboratory is operated by Triad National Security, LLC, for the National Nuclear Security Administration of U.S. Department of Energy (Contract No. 89233218CNA000001). Research presented in this poster was supported by the Laboratory Directed Research and Development program of Los Alamos National Laboratory under project number 20180238ER.

CONTACT INFORMATION

Please contact the author at msf@lanl.gov for more information.